Two-Photon-Triggered Drug Delivery in Cancer Cells Using Nanoimpellers**

Jonas Croissant, Marie Maynadier, Audrey Gallud, Harmel Peindy N'Dongo, Jeff L. Nyalosaso, Gaëlle Derrien, Clarence Charnay, Jean-Olivier Durand, Laurence Raehm, Françoise Serein-Spirau, Nathalie Cheminet, Thibaut Jarrosson, Olivier Mongin, Mireille Blanchard-Desce, Magali Gary-Bobo,* Marcel Garcia, Jie Lu, Fuyuhiko Tamanoi, Derrick Tarn, Tania M. Guardado-Alvarez, and Jeffrey I. Zink**

Nowadays, remote activation of nanoparticles (NPs) by light for biomedical applications has become an important area of research.[1] Among the different nano-objects, mesoporous silica nanoparticles (MSN) for light-triggered drug delivery applications have recently emerged and the field is expanding. Since the pioneering works of Zink,[2,3] Kim,[4] Lin,[5] and co-workers, many different systems have been described so far involving photocleavage,[4–11] photodissociation,[12] photoisomerization,[13–21] photorelease,[22] photothermal[23,24] photo-plasmonic heating,[25–28] and up-conversion photoisomerization.[29] Except for up-conversion, plasmonic and photothermal heating systems which can be activated with near-infrared (NIR) light, the majority of the studies is a proof-of-concept and was performed with UV/Vis light. Therefore the applications are limited because UV/Vis light can damage cells[30] and does not penetrate deep inside tissues. Using two-photon excitation (TPE) in the NIR region instead of UV/Vis light has many advantages such as deeper penetration in tissues (down to 2 cm), lower scattering losses, and three-dimensional spatial resolution. TPE is therefore highly suitable for applications in nanomedicine. Indeed nanomedicine aims at suppressing the side-effects of chemotherapeutic drugs, but the challenge to deliver on-demand such drugs with spatial and temporal accuracy remains unsolved. A two-photon actuated nanovehicle would provide an excellent spatial and temporal control of the release in tumors, which is not achieved with classical NIR systems. Only one example of photocleavage with MSN was described using TPE.[10] The drug was covalently attached to the MSN through the photocleavable linker, which necessitated the functionalization of the drug. Moreover, the MSN were tested on cancer cells with UV/Vis light.

Here, we report the synthesis of nanoimpellers[20] functionalized with a two-photon fluorophore F with a high two-photon absorption cross-section, suitable for Förster resonance energy transfer (FRET) to photoizomerize azobenzene A moieties in the NIR region (see Scheme 1). The nano-impeller groups pending in the porous framework allow the physical entrapment of the anticancer drug camptothecin, which is then kicked out of the pores by two-photon-triggered photoisomerization, and finally leads to in vitro cancer cell killing.

First, a novel fluorophore for TPE possessing two triethoxysilane moieties was designed and fully characterized (see the Supporting Information). The maximum fluorescence emission ($\lambda_{ex} = 385$ nm) of the fluorophore was 420 nm in tetrahydrofuran (THF), with a quantum yield of 88%.

The fluorophore or/and mono-triethoxysilylated azobenzene were co-condensed with tetraethoxysilane (TEOS) in basic media with cetyltrimethylammonium bromide (CTAB)

---

[*] J. Croissant, Dr. H. Peindy N'Dongo, Dr. J. L. Nyalosaso, Dr. G. Derrien, Dr. C. Charnay, Dr. J.-O. Durand, Dr. L. Raehm, Prof. F. Serein-Spirau, Dr. N. Cheminet, Dr. T. Jarrosson
Institut Charles Gerhardt Montpellier
UMR-5253 CNRS-UM2-ENSCM-UM1, cc 1701
Place Eugène Bataillon, 34095 Montpellier Cedex 05 (France)
E-mail: durand@um2.fr

Dr. M. Maynadier, A. Gallud, Dr. M. Gary-Bobo, Dr. M. Garcia
Institut des Biomolécules Max Mousseron UMR 5247 CNRS
Faculté de Pharmacie, 15 Avenue Charles Flahault
34093 Montpellier Cedex 05 (France)
E-mail: magali.gary-bobo@univ-montp1.fr

Dr. M. Blanchard-Desce
Université Bordeaux 1
Institut des Sciences Moléculaires, UMR CNRS 5255
351 Cours de la Libération, 33405 Talence Cedex (France)

Dr. O. Mongin
Institut Des Sciences Chimiques de Rennes
CNRS UMR 6226, Université Rennes 1
Campus Beaulieu, 35042 Rennes Cedex (France)

Dr. J. Lu, Prof. F. Tamanoi
Department of Microbiology, Immunology and Molecular Genetics
University of California Los Angeles
405 Hilgard Avenue, Los Angeles, CA 90095 (USA)

Dr. D. Tarn, T. M. Guardado-Alvarez, Prof. J. I. Zink
Department of Chemistry and Biochemistry
University of California Los Angeles
405 Hilgard Avenue, Los Angeles, CA 90095 (USA)
E-mail: zink@chem.ucla.edu
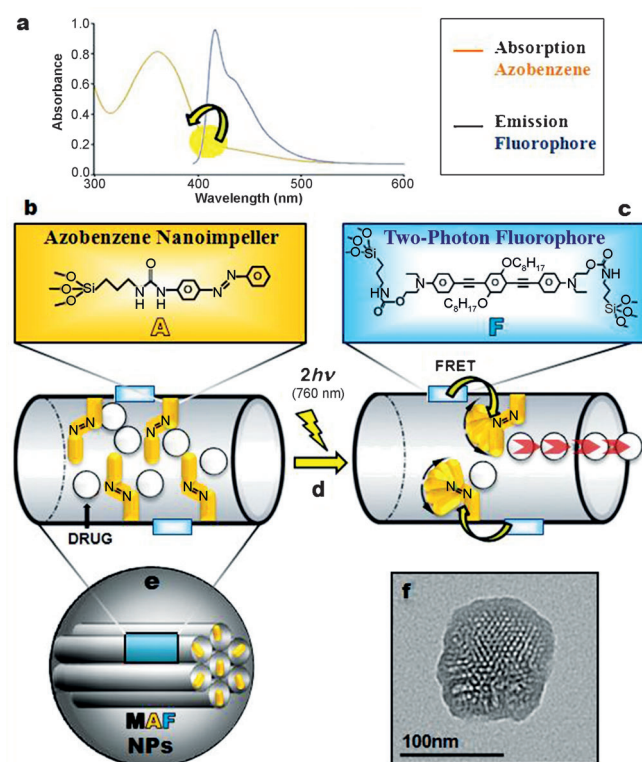
Scheme 1. Mesoporous silica nanoparticles combining b) azobenzene moieties A and c) a two-photon fluorophore F. The design of the so-called MAF nanoimpellers allows a two-photon (760 nm) activated release of drug molecules by a) FRET and d) photoisomerisation of azobenzene. e) Nanoimpellers and f) their transmission electron microscopy image.

following our synthesis procedure of MSN.[31] The as-prepared nanomaterials were labeled MA and MF, respectively for the mesoporous silica-azobenzene and mesoporous silica-fluorophore modification, whereas the co-condensation of both the azobenzene and the fluorophore with different proportions led to MAF-x (see Table 1).

Table 1: Characteristics of MA, MF, and MAF nanocarriers.

NPs	A/F Ratio	n_0 Azo [mol][a]	n_0 Fluo [mol][a]	S_{BET} [$m^2 g^{-1}$][a]
MA	–	3.7×10^{-4}	0	1144
MF	0	0	1.0×10^{-5}	991
MAF-1	0.8	4.0×10^{-5}	5.0×10^{-5}	1066
MAF-2	2.2	2.2×10^{-4}	1.0×10^{-4}	851
MAF-3	4.4	2.2×10^{-4}	5.0×10^{-5}	658
MAF-4	17.0	1.7×10^{-4}	1.0×10^{-5}	745

[a] Azo = azobenzene moieties, Fluo = fluorophore, and S_{BET} = Brunauer—Emmett—Teller surface.

The characterizations of the nanoimpellers after surfactant removal confirmed the nanosized mesoporous organosilicas (see Scheme 1d and Figures S1–S7 in the Supporting Information) with high specific surface areas suitable for cargo transportation.

FRET between the fluorophore and azobenzene moieties with MAF nanoimpellers was then studied by steady-state fluorescence experiments. First the fluorescence-emission quantum yield (Φ_F) of the fluorophore inside the MSN (MF sample) was determined to be 58%. The fluorescence emission of the MAF materials was quenched when the azobenzene groups were co-condensed with the fluorophore showing the FRET mechanism from the fluorophore to the azobenzene with MAF nanoimpellers (see Figure 1). When
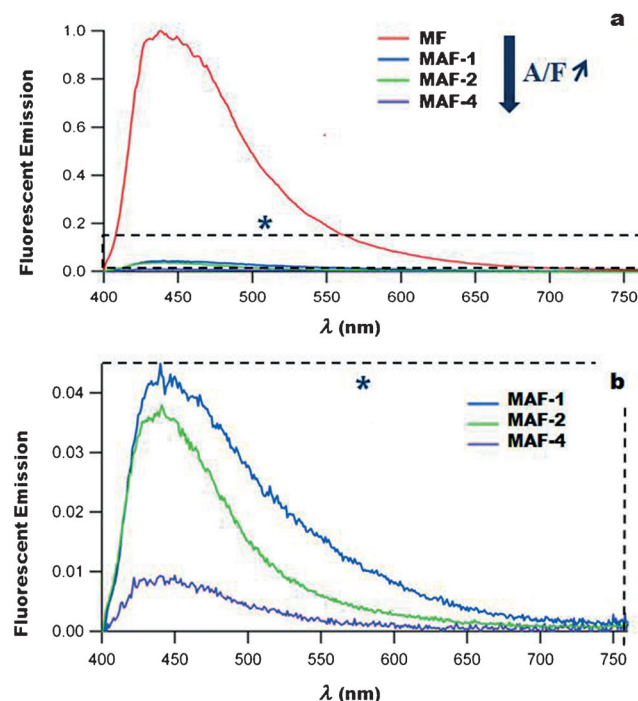

Figure 1. Fluorescence properties of MF and MAF nanoparticles ($\lambda_{ex} = 385$ nm). The fluorescence emission of the fluorophore which vanishes when the A/F ratio increases shows the energy transfer.

the A/F ratio increased the fluorescence quantum yield Φ_F decreased accordingly. The energy-transfer quantum yield (Φ_{ET}) increased and was maximum for MAF-4 (Table 2). The

Table 2: Photophysical properties of MA, MF, and MAF nanocarriers (Φ_F = fluorescence-emission quantum yield and Φ_{ET} = energy-transfer quantum yield).

NPs	$\lambda_{abs}/\lambda_{em}$ [nm]	Φ_F[a]	Φ_{ET}[a]	σ_2^{max}[b] [GM]
MA	368/–	0	–	–
MF	385/441	0.58	–	170
MAF-1	382/441	0.025	0.95	230
MAF-2	378/441	0.022	0.96	300
MAF-4	370/441	0.005	0.99	–

[a] Quinine bisulfate standard at 0.5 M in H_2SO_4. [b] Per chromophore.

same trend was observed in the work of Lo and co-workers[32] were fluorescein isothiocyanate was able to transfer its energy with a high quantum yield to a porphyrin photosensitizer, in MSN, for photodynamic TPE therapy. The two-photon absorption cross-sections σ_2 of the fluorophore and of MF and MAF samples were determined (Figure 2) and reached
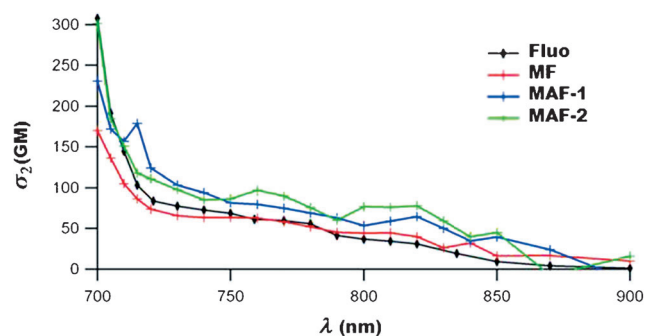
Figure 2. Two-photon absorption cross-sections of MF and MAF, compared with the fluorophore in ethanol.

a maximum at 700 nm. The two-photon absorption properties of the fluorophore were retained in the materials and no decrease of σ_2 was noticed after encapsulation.

The nanoimpellers MA and MAF were then loaded with rhodamine B (2 to 5% in mass), to give MA + R and MAF + R, respectively, in water to study cargo release under one-photon excitation. After centrifugation and extensive washing, the nanoparticles were put at the bottom of a quartz cell and the cell was carefully filled with water. The release of the cargo was monitored by UV/Vis spectroscopy (see Figure 3
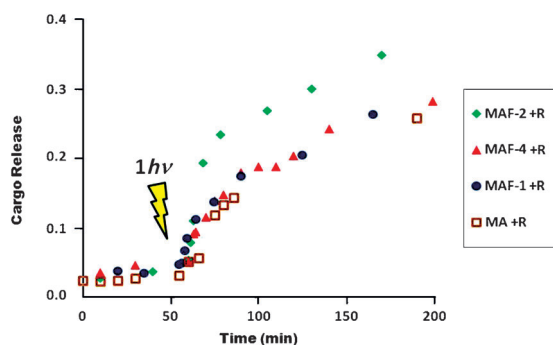

Figure 3. One-photon-triggered rhodamine B delivery in water. Comparison between nanoimpellers MA + R, MAF-1 + R, MAF-2 + R, and MAF-4 + R.

and Figure S8 in the Supporting Information). No release was noticed without irradiation. UV irradiation at 365 nm triggered the release of the cargo showing the efficiency of all the nanoimpellers in water.

The nanoimpellers were configured for two-photon activation, therefore an in vitro study was led on MCF-7 breast cancer cell line, and the laser excitation was performed with a Carl Zeiss two-photon confocal microscope. The cellular uptake was assessed by two-photon fluorescence imaging. The cell walls were stained with a cell mask 15 minutes before the imaging experiments. The remaining fluorescence of the fluorophore (Φ_F: 2.5 to 0.5%, see Table 2) was taken into advantage to localize the MAF nanoimpellers. The slight emission of MAF-3 and MAF-4 was localized within the cells thus demonstrating the successful internalization of the nanoimpellers (see Figure 4 and Figure S9).
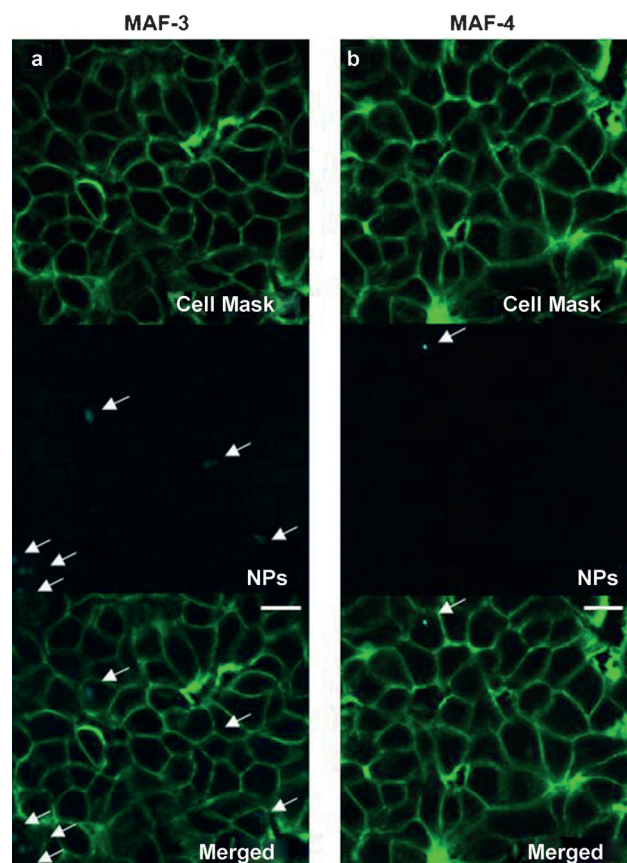

Figure 4. Two-photon fluorescence imaging of a) MAF-3, and b) MAF-4 confirming the cellular uptake of the nanoimpellers (the scale bars are 10 μm).

The nanoimpellers loaded with camptothecin (MA + C, MAF + C) were then screened under TPE in MCF-7 cancer cells. Cells were incubated with nanoimpellers in a 384 multiwell plate. Irradiation was performed with a Carl Zeiss microscope at very short time, with a focused laser beam and at maximum laser power (laser power input 3 W, laser power output before the objective 900 mW cm^{-2}). The well was irradiated with three scans of 1.57 s each per irradiated area, in four different areas, without overlaps between irradiated areas, with an objective: Carl Zeiss numerical aperture 0.3, 10-fold magnification. Half of the well was irradiated with this technique. The MTT assay was performed two days after irradiation. MA, MF, and MAF-4 nanoparticles did not induce cell death, with or without irradiation in the absence of camptothecin (see Figure S11). We further verify the safety of these nanoparticles by a incubation time of 4 days with increasing dose of MAF-4 on normal fibroblasts and MCF-7 cancer cells (Figure S10). Nanoimpellers were thus not toxic for cells and direct cancer cell killing (photothermal effect or ROS generation) was not observed. When loaded with camptothecin, MAF-1 + C and MAF-2 + C did not induce more killing of cancer cells under TPE than without irradiation which is probably correlated to the low A/F ratio (Figure 5 a). By contrast, when the A/F ratio increased, more cancer cell death was observed with MAF-3 + C and MAF-
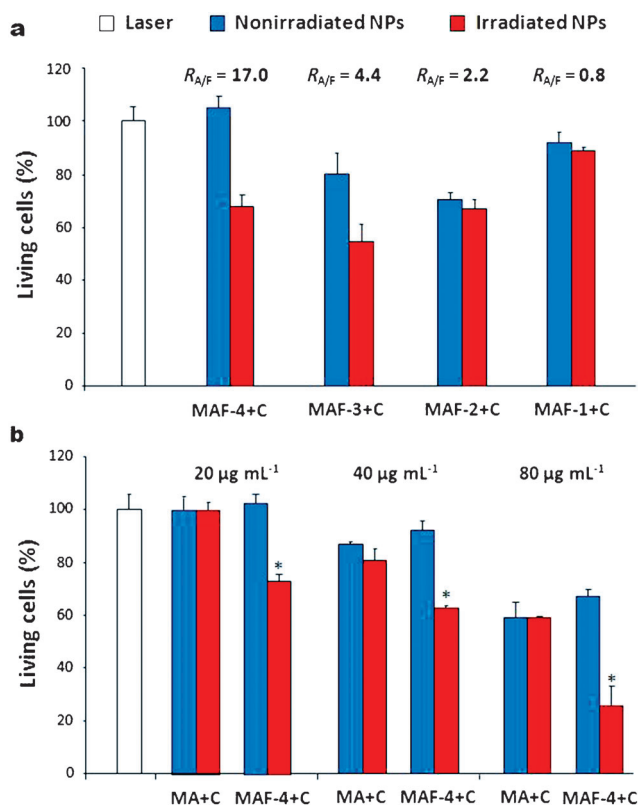
Figure 5. Two-photon-triggered in vitro delivery of camptothecin, comparison between a) nanoimpellers MAF-1+C, 2+C, 3+C, 4+C, at 20 μg mL^{-1} and b) MA and MAF-4 at 20–80 μg mL^{-1}. Data are mean values ± standard deviation from three independent experiments. * Statistically significant versus nonirradiated nanoparticles ($p < 0.05$ from Student's t test; $R_{A/F} = A/F$ ratio).

4 + C nanoimpellers under TPE than without irradiation, and the best result was obtained with MAF-4 + C nanoimpeller possessing an A/F ratio of 17 and a high energy-transfer quantum yield (see ESI S9).

Hence, further in vitro experiments were led at different concentrations (from 20 to 80 μg mL^{-1}) with MA + C and MAF-4 + C nanoimpellers (Figure 5b). MA + C nanoimpeller which does not possess the two-photon fluorophore did not kill cancer cells under TPE (see Figure 5b) at 20 μg mL^{-1} and no difference was observed between irradiated and nonirradiated cells with MA + C nanoimpeller at higher concentration. By contrast MAF-4 + C nanoimpeller was efficient in killing cancer cells at 20 and 40 μg mL^{-1}, under TPE and up to 40% of cancer cell death was observed. At 80 μg mL^{-1} MAF-4 + C nanoimpeller induced 30% of cancer cell death without irradiation and 75% cell death with irradiation. These results demonstrate that the fluorophore was necessary to observe cancer cell death with nanoimpellers under TPE at short time of irradiation, focused laser beam and high power. Note that MA + C and MAF-4 + C were both efficient in inducing cancer cell killing under different conditions for TPE (Figures S12–S13). Furthermore, premature release of camptothecin was not observed in aqueous solution without irradiation (Figure S14).

In conclusion, we have designed nanoimpellers with a two-photon fluorophore possessing a high two-photon absorption cross-section, leading to nanoimpellers configured for TPE with FRET from the fluorophore to the azobenzene. The residual fluorescence of the nanoimpellers allowed to perform TPE fluorescence imaging in cancer cells demonstrating the internalization of the nanoimpellers. Nanoimpeller MAF-4 + C with a high energy transfer quantum yield from the fluorophore to the azobenzene moiety was able to induce cancer cell death under these TPE conditions and was not toxic to cells without irradiation at low concentration. Work is in progress to further extend the scope and applications of this methodology.

Experimental Section

Two-photon Induced drug delivery: Human breast cancer cells MCF-7 (purchased from ATCC) were cultured in Dulbecco's Modified Eagle's Medium (DMEM) supplemented with 10% fetal bovine serum and 50 μg mL^{-1} gentamycin. All cells were allowed to grow in humidified atmosphere at 37°C under 5% CO_2. For in vitro phototoxicity, MCF-7 cells were seeded into a 384 multiwell glass-bottomed plate (thickness 0.17 mm), with a black polystyrene frame, 2000 cells per well in 50 μL of culture medium, and allowed to grow for 24 h. Nanoimpellers loaded with camptothecin were then dispersed under ultrasound in phosphate-buffered saline (PBS) at a concentration of 1 mg mL^{-1} and cells were then incubated for 20 h with or without nanoimpellers at a final concentration of 20 to 80 μg mL^{-1} in DMEM. After incubation with nanoimpellers, the cells were washed twice, maintained in fresh culture medium, and then submitted (or not) to laser irradiation using the Carl Zeiss Microscope (laser power input 3 W). Half of the well was irradiated at 760 nm by three scans of 1.57 s duration in four different areas of the well. The laser beam was focused by a microscope objective lens (Carl Zeiss 10-fold magnification/objective 0.3 EC Plan-Neofluar). The scan size does not allow irradiating more areas without overlapping. After 2 days, the MTS (3-(4,5-dimethylthiazol-2-yl)-5-(3-carboxymethoxyphenyl)-2-(4-sulfonyl)-2H-tetrazolium) colorimetric bioassay was performed (as previously described) and was corrected according to the following formula Abs$_{control}$−2(Abs$_{control}$−Abs$_{Nanoimpellers}$) where Abs is absorption.

[1] R. Tong, D. S. Kohane, *Wiley Interdiscip. Rev. Nanomed. Nanobiotechnol.* **2012**, *4*, 638–662.

[2] E. Johansson, E. Choi, S. Angelos, M. Liong, J. I. Zink, *J. Sol-Gel Sci. Technol.* **2008**, *46*, 313–322.

[3] T. D. Nguyen, K. C. F. Leung, M. Liong, Y. Liu, F. Stoddart, J. I. Zink, *Adv. Funct. Mater.* **2007**, *17*, 2101–2110.

[4] C. Park, K. Lee, C. Kim, *Angew. Chem.* **2009**, *121*, 1301–1304; *Angew. Chem. Int. Ed.* **2009**, *48*, 1275–1278.

[5] J. L. Vivero-Escoto, I. I. Slowing, C. W. Wu, V. S. Y. Lin, *J. Am. Chem. Soc.* **2009**, *131*, 3462–3463.

[6] N. Ž. Knežević, V. S. Y. Lin, *Nanoscale* **2013**, *5*, 1544–1551.

[7] D. He, X. He, K. Wang, J. Cao, Y. Zhao, *Langmuir* **2012**, *28*, 4003–4008.

[8] A. Agostini, F. Sancenon, R. Martinez-Manez, M. D. Marcos, J. Soto, P. Amoros, *Chem. Eur. J.* **2012**, *18*, 12218–12221.

[9] N. Ž. Knežević, B. G. Trewyn, V. S. Y. Lin, *Chem. Eur. J.* **2011**, *17*, 3338–3342.

[10] Q. N. Lin, Q. Huang, C. Y. Li, C. Y. Bao, Z. Z. Liu, F. Y. Li, L. Y. Zhu, *J. Am. Chem. Soc.* **2010**, *132*, 10645–10647.

[11] J. Lai, X. Mu, Y. Xu, X. Wu, C. Wu, C. Li, J. Chen, Y. Zhao, *Chem. Commun.* **2010**, *46*, 7370–7372.

[12] D. He, X. He, K. Wang, J. Cao, Y. Zhao, *Adv. Funct. Mater.* **2012**, *22*, 4704–4710.

[13] Y. Wang, B. Li, L. Zhang, H. Song, L. Zhang, *Acs Appl. Mater. Interfaces* **2013**, *5*, 11–15.

[14] Q. Yuan, Y. Zhang, T. Chen, D. Lu, Z. Zhao, X. Zhang, Z. Li, C.-H. Yan, W. Tan, *Acs Nano* **2012**, *6*, 6337–6344.

[15] H. Yan, C. Teh, S. Sreejith, L. Zhu, A. Kwok, W. Fang, X. Ma, N. Kim Truc, V. Korzh, Y. Zhao, *Angew. Chem.* **2012**, *124*, 8498–8502; *Angew. Chem. Int. Ed.* **2012**, *51*, 8373–8377.

[16] Y. Wen, L. Xu, W. Wang, D. Wang, H. Du, X. Zhang, *Nanoscale* **2012**, *4*, 4473–4476.

[17] X. Mei, S. Yang, D. Chen, N. Li, H. Li, Q. Xu, J. Ge, J. Lu, *Chem. Commun.* **2012**, *48*, 10010–10012.

[18] Y. A. Lau, B. L. Henderson, J. Lu, D. P. Ferris, F. Tamanoi, J. I. Zink, *Nanoscale* **2012**, *4*, 3482–3489.

[19] D. P. Ferris, Y. L. Zhao, N. M. Khashab, H. A. Khatib, J. F. Stoddart, J. I. Zink, *J. Am. Chem. Soc.* **2009**, *131*, 1686–1688.

[20] J. Lu, E. Choi, F. Tamanoi, J. I. Zink, *Small* **2008**, *4*, 421–426.

[21] S. Angelos, E. Choi, F. Voegtle, L. De Cola, J. I. Zink, *J. Phys. Chem. C* **2007**, *111*, 6589–6592.

[22] N. Ž. Kneževic, B. G. Trewyn, V. S. Y. Lin, *Chem. Commun.* **2011**, *47*, 2817–2819.

[23] A. K. Singh, M. A. Hahn, L. G. Gutwein, M. C. Rule, J. A. Knapik, B. M. Moudgil, S. R. Grobmyer, S. C. Brown, *Int. J. Nanomed.* **2012**, *7*, 2739–2750.

[24] L. G. Gutwein, A. K. Singh, M. A. Hahn, M. C. Rule, J. A. Knapik, B. M. Moudgil, S. C. Brown, S. R. Grobmyer, *Int. J. Nanomed.* **2012**, *7*, 351–357.

[25] Z. Jiang, B. Dong, B. Chen, J. Wang, L. Xu, S. Zhang, H. Song, *Small* **2013**, *9*, 604–612.

[26] Z. Zhang, L. Wang, J. Wang, X. Jiang, X. Li, Z. Hu, Y. Ji, X. Wu, C. Chen, *Adv. Mater.* **2012**, *24*, 1418–1423.

[27] X. Yang, X. Liu, Z. Liu, F. Pu, J. Ren, X. Qu, *Adv. Mater.* **2012**, *24*, 2890–2895.

[28] J. Croissant, J. I. Zink, *J. Am. Chem. Soc.* **2012**, *134*, 7628–7631.

[29] J. Liu, W. Bu, L. Pan, J. Shi, *Angew. Chem.* **2013**, *125*, 4471–4475; *Angew. Chem. Int. Ed.* **2013**, *52*, 4375–4379.

[30] T. Kushibiki, T. Hirasawa, S. Okawa, M. Ishihara, *Photomed. Laser Surgery* **2013**, *31*, 95–104.

[31] M. Gary-Bobo, Y. Mir, C. Rouxel, D. Brevet, I. Basile, M. Maynadier, O. Vaillant, O. Mongin, M. Blanchard-Desce, A. Morere, M. Garcia, J.-O. Durand, L. Raehm, *Angew. Chem.* **2011**, *123*, 11627–11631; *Angew. Chem. Int. Ed.* **2011**, *50*, 11425–11429.

[32] S.-H. Cheng, C.-C. Hsieh, N.-T. Chen, C.-H. Chu, C.-M. Huang, P.-T. Chou, F.-G. Tseng, C.-S. Yang, C.-Y. Mou, L.-W. Lo, *Nano Today* **2011**, *6*, 552–563.